CHALMERS
UNIVERSITY OF TECHNOLOGY

Detecting itinerant single microwave photons

C. R. Physique 17 (2016) 756–765

Contents lists available at ScienceDirect

Comptes Rendus Physique

www.sciencedirect.com

Quantum microwaves / Micro-ondes quantiques

Detecting itinerant single microwave photons

Détection de photons micro-ondes itinérants

Sankar Raman Sathyamoorthy [a,*], Thomas M. Stace [b], Göran Johansson [a]

[a] *Department of Microtechnology and Nanoscience, MC2, Chalmers University of Technology, SE-41296 Gothenburg, Sweden*
[b] *Centre for Engineered Quantum Systems, School of Physical Sciences, University of Queensland, Saint Lucia, Queensland 4072, Australia*

ARTICLE INFO

Article history:
Available online 3 August 2016

Keywords:
Single-photon detection
Quantum nondemolition
Superconducting circuits
Microwave photons

Mots-clés :
Détection de photons uniques
Mesure quantique non destructive
Circuits supraconducteurs
Photons micro-ondes

ABSTRACT

Single-photon detectors are fundamental tools of investigation in quantum optics and play a central role in measurement theory and quantum informatics. Photodetectors based on different technologies exist at optical frequencies and much effort is currently being spent on pushing their efficiencies to meet the demands coming from the quantum computing and quantum communication proposals. In the microwave regime, however, a single-photon detector has remained elusive, although several theoretical proposals have been put forth. In this article, we review these recent proposals, especially focusing on non-destructive detectors of propagating microwave photons. These detection schemes using superconducting artificial atoms can reach detection efficiencies of 90% with the existing technologies and are ripe for experimental investigations.

RÉSUMÉ

Les détecteurs de photons uniques sont des outils fondamentaux en optique quantique et tiennent un rôle central dans la théorie de la mesure et l'informatique quantique. Dans le domaine optique, plusieurs types de photo-détecteurs sont opérationnels et, pour répondre aux exigences du calcul et de la communication quantiques, un effort considérable est actuellement porté sur l'amélioration de leurs efficacités. Cependant, dans le domaine des micro-ondes, la détection de photons uniques reste un défi à relever, bien que plusieurs propositions théoriques aient été faites. Dans cet article, nous passerons en revue ces récentes propositions, avec un accent particulier sur la détection non destructive de photons mico-ondes propagatifs. Ces schémas de détection basés sur des atomes artificiels supraconducteurs peuvent atteindre des efficacités de détection de 90% avec des technologies existantes et sont prêts pour l'expérimentation.

* Corresponding author.
E-mail addresses: sankarr@chalmers.se (S.R. Sathyamoorthy), goran.l.johansson@chalmers.se (G. Johansson).

http://dx.doi.org/10.1016/j.crhy.2016.07.010
1631-0705/

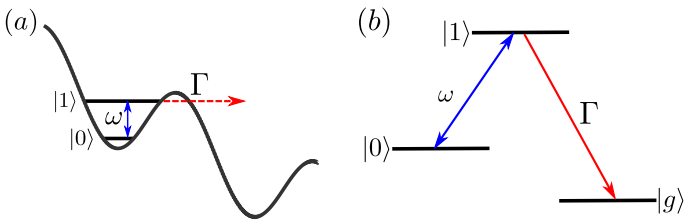

Fig. 1. (a) Tilted washboard potential of a current biased Josephson junction. The bias current I_b is chosen such that only two energy levels exist within each well. (b) A Λ three-level system that maps to the spectrum shown in (a).

1. Introduction

In 1905, his *annus mirabilis*, Einstein not only postulated the existence of light quanta (photons) while explaining the photoelectric effect, but also gave a theory (arguably the first) of a photon detector [1]. In the decades that followed, significant progress was made in designing photon detectors based on several technologies such as photomultiplier tubes, avalanche photodiodes and cryogenic detectors, among others. Such detectors are routinely used in experimental setups in applications ranging from spectroscopy to sensors. Recently, there has been a huge drive coming from the field of quantum information processing to push the efficiency of photon detectors to work at the quantum limit. An ideal photon detector is expected to have 100% efficiency, a very low dark count and a number resolving nature. Such high-efficiency single-photon detectors are crucial in the implementation of quantum cryptography proposals such as quantum key distribution (QKD) [2], in experimental tests of the foundations of quantum mechanics such as Bell tests [3] and in implementing all optical quantum computers [4] among several other applications. Several single-photon detectors have been realized in the optical regime [5,6] and are part of the standard quantum optics toolkit. However, single-photon detectors at microwave frequencies have been difficult to implement, and researchers have resorted to special schemes for homodyne and correlation measurements [7,8]. The focus of this article is to review some of the proposals that have been put forth to fill this gap.

Of particular interest among photodetectors are the non-destructive ones. These detectors are transparent to the incoming photons and the measurement scheme is termed as quantum nondemolition (QND). QND measurements were first proposed to detect gravitational waves by evading the measurement back-action on the system [9–13]. These measurement schemes were well suited for the field of quantum optics, leading to the successful implementation of QND measurements of photon flux in the optical regime [14]. QND detectors play a major role in schemes such as quantum error correction [15], state preparation by measurement [16,17], and one-way quantum computing [18]. We will focus on recent proposals for the nondestructive detection of microwave photons in section 3.

We have to note, nevertheless, that photon detection schemes (including QND detection) have been shown earlier for microwaves stored in cavities [19–23]. While strong interactions could be mediated between the photons in the cavity and matter used as a detector, the use of cavities also complicates the setup as one has to worry about the bandwidth of operation and the compromise between quality factor and reflection. Schemes to catch microwave photons in a cavity by tuning their coupling with a transmission line have been developed recently [24–26]. However, one has to know the exact shape, width and the arrival time of the wave-packet to completely absorb the photon into the cavity. These additional problems make such schemes less attractive for applications such as those discussed above. Hence, in this review, we will focus on detectors designed for propagating microwave photons.

The article is organized as follows. In section 2, we will discuss proposals for microwave photon detection that are destructive in nature. These proposals are based on current biased Josephson junctions (CBJJ). In the next section, we will look at proposals that use photon–photon interactions mediated by a superconducting artificial atom to perform the QND detection of microwave photons. In the final section, we will summarize the main messages from these proposals.

2. Photon detectors based on Josephson junctions

Initial proposals for detecting propagating microwave photons were based on current biased Josephson junctions (CBJJ) [27–29]. These junctions have a potential energy $U(\delta) = -(I_c\Phi_0/2\pi)\cos(\delta) - I_b\delta$, where I_c is the critical current of the junction, $\Phi_0 = h/2e$ is the flux quantum and δ is the superconducting phase difference across the junction. Such a potential, known as a tilted washboard potential (see Fig. 1a), has several local minima or potential wells that have a discrete set of states. We can tune the potential barrier of the local minima and the number of allowed energy levels using the bias current I_b. For a particular value of I_b (depending on I_c), each of the wells acts as a two-level system that can be used as a qubit. The lifetimes of these levels $|0\rangle$ and $|1\rangle$ depend on the tunneling distance to the continuum of modes to the right. As seen from the figure, the tunneling from $|0\rangle$ is exponentially suppressed compared to the decay from the state $|1\rangle$. If we neglect the tunneling from the state $|0\rangle$, the setup can be mapped to a three-level Λ system (Fig. 1(b)), with $|1\rangle$ being a metastable state with a short lifetime set by the rate Γ. The incoming photon with a frequency close to the transition frequency ω excites the qubit to the state $|1\rangle$. The excitation from $|1\rangle$ decays irreversibly with the rate Γ into the continuum that is labeled here as the state $|g\rangle$. This leads to a voltage drop across the junction that can be measured classically and the excitation is lost, making this a destructive scheme.

The performance of the detector is characterized by the probability of absorption of the incoming photon. This is theoretically calculated as follows. We start with the non-Hermitian Hamiltonian of the Λ system in the real space representation ($\hbar = 1$) [29]

$$H = (\omega - \mathrm{i}\,\Gamma/2)\,|1\rangle\langle 1| + \mathrm{i}\,v_{\mathrm{g}} \int \mathrm{d}x \left(\psi_{\mathrm{L}}^{\dagger}\partial_x\psi_{\mathrm{L}} - \psi_{\mathrm{R}}^{\dagger}\partial_x\psi_{\mathrm{R}}\right) + V \int \mathrm{d}x\,\delta(x)\left[(\psi_{\mathrm{R}} + \psi_{\mathrm{L}})\,|1\rangle\langle 0| + \mathrm{h.c.}\right] \tag{1}$$

where $\psi_{\mathrm{R/L}}$ is the radiation field traveling right/left with a group velocity v_{g}. The interaction between the photons and the Λ system is modeled as a delta potential of strength V at $x = 0$. A general single-excitation wave-function of the total system is of the form [29]

$$|\phi\rangle = \int \mathrm{d}x \left[\xi_{\mathrm{R}}(x,t)\psi_{\mathrm{R}}^{\dagger}(x) + \xi_{L}(x,t)\psi_{\mathrm{L}}^{\dagger}(x)\right]|0,\mathrm{vac}\rangle + e(t)\,|1,\mathrm{vac}\rangle \tag{2}$$

where $|0,\mathrm{vac}\rangle$ is the state with the Λ system in the state $|0\rangle$ and the radiation field in vacuum. The single photon wavepackets are given by $\xi_{R/L}(x,t)$. Solving the Schrödinger equation for the above Hamiltonian with this state, we get three coupled equations for the coefficients $\xi_{\mathrm{R}}(x,t)$, $\xi_{\mathrm{L}}(x,t)$ and $e(t)$. From the solution of these coupled equations, the probability of level $|g\rangle$ can be calculated as $P_g = 1 - \|\phi\|^2$. The value of this probability at long times is taken as the measure the detector efficiency. With the Λ system in the middle of an open transmission line, the maximum attainable efficiency was calculated to be 50% [27]. This could be improved by having several such scatterers along the line, which also increased the bandwidth of operation. In [29], it was theoretically shown that by placing one atom at the end of the transmission line (in front of a mirror), the efficiency could be increased to 100%.

The above-discussed analysis was done for an ideal Λ system, of which the CBJJ is only an approximation. While tunneling from the state $|0\rangle$ is much smaller than tunneling from the state $|1\rangle$, it is not zero. Direct tunneling from the ground state $|0\rangle$ leads to dark counts, which affects the performance of the setup. The performance of CBJJ as a photodetector (referred to as Josephson photomultiplier (JPM) in the following references to distinguish it from phase qubits that ideally work at different parameter regimes) was analyzed both experimentally and theoretically, including the direct tunneling from the state $|0\rangle$ in references [30–33]. However, these works are primarily aimed at measuring the photon occupation number inside a cavity. Further analysis is needed to check the efficiency of such a system to be used as a detector for itinerant single photons.

During the late stage of preparation of this manuscript, we note that a different Λ system based on a driven superconducting qubit dispersively coupled with a resonator was proposed and theoretically analyzed for single-microwave photon detection, in both time-gated and continuous modes of operation [34,35]. Even more recently, such a setup has also been experimentally demonstrated in the time-gated mode, with a photon detection efficiency around 0.66 [36].

3. QND detection of itinerant microwave photons

3.1. A transmon in a transmission line

The transmon [37], a widely used superconducting artificial atom, is a single Cooper pair box shunted with a capacitance C_{S}. The large shunt capacitance reduces the charging energy E_{C} of the circuit and thereby also the sensitivity of the qubit to charge noise, which is one of the main reasons for the transmon's popularity. Recently, it was shown that a transmon could behave as a Kerr medium that imparts a giant conditional phase shift on microwave fields incident on the atom [38]. Following schemes for the QND detection of photons based on the cross-Kerr effect in the optical regime, proposals for nondestructive single-photon detection in the microwave frequencies using the transmon were analyzed in references [39–41]. We will briefly review these setups in this section.

For the purpose of this article, we will consider the transmon as essentially a three-level system with the Hamiltonian ($\hbar = 1$)

$$H = -\omega_{01}\,|0\rangle\langle 0| + \omega_{12}\,|2\rangle\langle 2| \tag{3}$$

where $\omega_{ij} = E_j - E_i$ is the energy difference between levels i and j. The 1–2 transition is driven by a coherent probe field with frequency ω_{p} and amplitude α_p. The 0–1 transition is driven by the control field of frequency ω_c which contains either 0 or 1 photon (see Fig. 2). In the rotating frame of the input fields, the Hamiltonian can be written including the coherent drive as

$$H = -\Delta_c\,|0\rangle\langle 0| + \Delta_p\,|2\rangle\langle 2| + \Omega_{\mathrm{p}}(L_{12} + L_{21}) \tag{4}$$

where the detunings $\Delta_c = \omega_{01} - \omega_c$, $\Delta_p = \omega_{12} - \omega_{\mathrm{p}}$ and we have taken $\alpha_{\mathrm{p}} = \mathrm{i}\,\Omega_{\mathrm{p}}$, with a real Ω_{p}. We also denote the coupling operators as $L_{ij} = \sqrt{\Gamma_{ij}}\,|i\rangle\langle j|$, where Γ_{ij} is the decay rate from jth energy level to ith level. The above Hamiltonian is valid for an atom with one input–output port. Such a setup can be achieved by placing the transmon at the end of a semi-infinite transmission line. With the transmon initially in the ground state $|0\rangle$, the probe field does not interact with the 1–2 transition. The probe field is scattered only when the control field has a photon that excites the transmon to the state $|1\rangle$. By monitoring the output probe field using homodyne detection, the presence of the single control photon can thus be inferred.

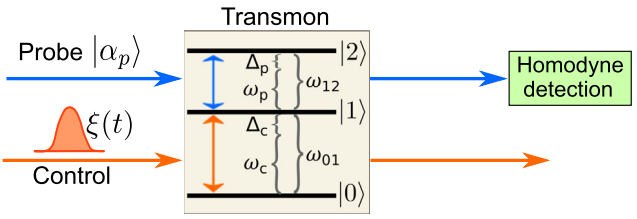

Fig. 2. A scheme for single-photon detection using a single three-level system. Such a setup could be achieved in superconducting circuits with a transmon at the end of a transmission line. The difference in the homodyne current with and without a single control photon in the wave-packet $\xi(t)$ constitutes the signal.

The single photon in the control field can be modeled as the output from a fictitious cavity with damping rate $\kappa(t)$. By modulating $\kappa(t) = \xi(t)/\sqrt{\int_t^\infty |\xi(s)|^2\,\mathrm{d}s}$, the shape of the temporal wave packet $\xi(t)$ containing the single photon can be set arbitrarily [42]. The master equation of the setup is

$$\begin{aligned}\dot{\rho} &= -\mathrm{i}\,[H,\rho] + (\mathcal{D}[L_{01}] + \mathcal{D}[L_{12}])\,\rho + \kappa(t)\mathcal{D}[a]\,\rho - \sqrt{\kappa(t)}\,\mathcal{C}[a, L_{01}]\,\rho \\ &\equiv \mathcal{L}_{\mathrm{cav}}\,\rho \end{aligned} \tag{5}$$

where ρ is the total density matrix of the source cavity and the transmon, a ($a^\dagger$) is the annihilation (creation) operator for the photons in the cavity and the dissipation super-operator is given by $\mathcal{D}[c]\,\rho = c\rho c^\dagger - \frac{1}{2}c^\dagger c\rho - \frac{1}{2}\rho c^\dagger c$. We have also defined a Liouvillian $\mathcal{L}_{\mathrm{cav}}$ and a coupling super-operator $\mathcal{C}[c_1, c_2]\,\rho = \left[c_2^\dagger, c_1\rho\right] + \left[\rho\, c_1^\dagger, c_2\right]$ for shorthand.

The output probe field that is measured using the homodyne detector is given by the standard input–output formalism as $\Omega_{\mathrm{p,out}} = \Omega_{\mathrm{p}} + L_{12}$. However, we are only interested in the change of the probe field with and without a single photon in the control field, i.e. only on L_{12}. The interesting part of the homodyne current can thus be defined as

$$j(t)\mathrm{d}t = \sqrt{\eta}\left\langle \mathrm{e}^{\mathrm{i}\phi}L_{12}(t) + \mathrm{e}^{-\mathrm{i}\phi}L_{21}(t)\right\rangle \mathrm{d}t + \mathrm{d}W(t) \tag{6}$$

where $0 \le \eta \le 1$ is the efficiency of the homodyne detector and ϕ is the phase of the local oscillator that specifies the quadrature of the measurement. $\mathrm{d}W(t)$ is a Wiener increment with a mean $E[\mathrm{d}W(t)] = 0$ and variance $E[\mathrm{d}W(t)^2] = \mathrm{d}t$, where $E[\cdot]$ is the ensemble average. To convert the above time trace of the homodyne current into a binary flag, we define a signal $S = \int_{t_\mathrm{i}}^{t_\mathrm{f}} j(t) f(t)\,\mathrm{d}t$, where $t_\mathrm{m} = t_\mathrm{f} - t_\mathrm{i}$ is the measurement time window and $f(t)$ is a linear filter function. We will initially take $f(t)$ to be just a square pulse with value 1 when $t_\mathrm{i} \le t \le t_\mathrm{f}$ and 0 otherwise.

To characterize the performance of this setup as a photon detector, we can define the signal-to-noise ratio (SNR) as

$$SNR = \frac{E[S_1] - E[S_0]}{\sqrt{\mathrm{Var}[S_1] + \mathrm{Var}[S_0]}} \tag{7}$$

where $S_{0/1}$ is the signal with 0 or 1 photon in the control field and $\mathrm{Var}[X] = E[X^2] - E[X]^2$ is the variance. The SNR can be calculated from the above master equation (5). The average and variance in this case are

$$\begin{aligned} E[S_0] &= 0 \\ E[S_0^2] &= t_\mathrm{m} \\ E[S_1] &= \sqrt{\eta}\int_{t_i}^{t_f} \langle \hat{y}\rangle\,\mathrm{d}t \\ E[S_1^2] &= \int_{t_i}^{t_f}\mathrm{d}t_1 \int_{t_i}^{t_f}\mathrm{d}t_2\; E[j(t_1)j(t_2)] \end{aligned} \tag{8}$$

The two-time-correlation function can be evaluated using the quantum regression theorem [43] as

$$\begin{aligned} E[j(t_1)j(t_2)] = \Theta(t_2 - t_1)\Big(\eta\mathrm{Tr}\left((\mathrm{e}^{\mathrm{i}\phi}L_{12} + \mathrm{e}^{-\mathrm{i}\phi}L_{21})\mathcal{T}(t_2 - t_1)(\mathrm{e}^{\mathrm{i}\phi}L_{12}\rho(t_1) + \mathrm{e}^{-\mathrm{i}\phi}\rho(t_1)L_{21})\right) + \delta(t_2 - t_1)\Big) \\ + \Theta(t_1 - t_2)\Big(\eta\mathrm{Tr}\left((\mathrm{e}^{\mathrm{i}\phi}L_{12} + \mathrm{e}^{-\mathrm{i}\phi}L_{21})\mathcal{T}(t_1 - t_2)(\mathrm{e}^{\mathrm{i}\phi}L_{12}\rho(t_2) + \mathrm{e}^{-\mathrm{i}\phi}\rho(t_2)L_{21})\right) + \delta(t_1 - t_2)\Big) \end{aligned} \tag{9}$$

where $\mathcal{T}(t_2 - t_1)\mathbb{Y}(t_1) = \mathbb{Y}(t_2)$ with $\mathbb{Y}(t) = \mathrm{e}^{\mathrm{i}\phi}L_{12}\rho(t) + \mathrm{e}^{-\mathrm{i}\phi}\rho(t)L_{21}$. The time evolution operator $\mathcal{T}(t_2 - t_1)$ is evaluated by solving $\dot{\mathbb{Y}} = \mathcal{L}_{\mathrm{cav}}\mathbb{Y}$. By definition, the step function $\Theta(t) = 0$ for $t < 0$ and 1 otherwise.

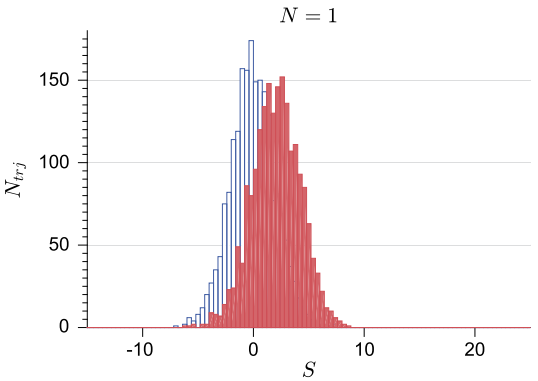

Fig. 3. Histogram of the integrated homodyne current S with (red) and without (blue) a photon in the control field, using a single transmon ($N = 1$) at the end of a transmission line. The number of trajectories in both cases ($n = 0$ and $n = 1$ control photons) was 2000. The parameters used in the units of Γ_{01} are $\Delta_{01} = \Delta_{12} = 0, \Omega_{\rm p} = 0.35$ and $\Gamma_{12} = 2$, while the quadrature of measurement is set with $\phi = \pi/2$. The input control photon is of Gaussian temporal shape with $\Gamma_{ph} = 0.8$ and $T_{ph} = 4$. The time of measurement $t_{\rm m}$ was optimized to give the best SNR. As is evident from the distribution, the SNR in this case is less than 1.

The signal-to-noise ratio is an ideal measure for Gaussian statistics, but is not necessarily a good measure for other distributions that need higher-order moments for complete description. In order to collect such statistics of the signal distribution and define more relevant measures, we use the formalism of stochastic master equations (SMEs). These equations describe the evolution of the system under measurements and can be considered as an unraveling of the average system dynamics described by the master equation (5) [45]. With the tunable cavity as the photon source, the SME is given by

$$\mathrm{d}\rho = \mathcal{L}_{\rm cav}\,\rho\,\mathrm{d}t + \sqrt{\eta}\mathcal{M}[L_{12}]\,\rho\,\mathrm{d}W(t) \tag{10}$$

where we have defined a measurement super-operator $\mathcal{M}[c]\,\rho = (\mathrm{e}^{\mathrm{i}\phi}c\rho + \mathrm{e}^{-\mathrm{i}\phi}\rho c^\dagger) - \langle \mathrm{e}^{\mathrm{i}\phi}c + \mathrm{e}^{-\mathrm{i}\phi}c^\dagger\rangle\rho$, which describes the back-action of the measurement on the evolution of the system [44].

To get the distribution of the signal, we numerically solve the above equations with $n = 0$ and $n = 1$ photon in the control field. Each run of this simulation is called a trajectory and gives a particular value of S. The number of trajectories should be high enough to get a probability distribution for S. In this case, we can define the fidelity of single-photon detection as

$$F = P(0|S \le S_0^{\rm T})P(S \le S_0^{\rm T}) + P(1|S \ge S_1^{\rm T})P(S \ge S_1^{\rm T}) \tag{11}$$

where $P(0|S \le S_0^{\rm T})$ is the conditional probability to have 0 photons in the control field given that the measured integrated current S was found to be less than or equal to a predefined threshold $S_0^{\rm T}$. $P(1|S \ge S_1^{\rm T})$ is defined analogously.

As first shown in [39], the signal generated using a single transmon in the above setup cannot overcome the quantum noise. This can be seen from the distribution of the signal shown in Fig. 3, which is obtained from the numerical simulation of the above stochastic master equations. The distribution is obtained from 2000 trajectories for $n = 0$ and $n = 1$ control photons, assuming no additional losses such as dephasing in the transmon and with perfect homodyne detection ($\eta = 1$). In this simulation, we have also taken the single photon to be in a Gaussian wave-packet given by

$$\xi(t) = \left(\frac{\Gamma_{\rm ph}^2}{2\pi}\right)^{1/4} \exp\left(\frac{-\Gamma_{\rm ph}^2(t - T_{\rm ph})^2}{4}\right)$$

where $\Gamma_{\rm ph}$ gives the width of the wave packet and $T_{\rm ph}$ is the time of arrival of the peak of the wave packet to the transmon, with the normalization condition $\int |\xi(t)|^2 \mathrm{d}t = 1$. The parameter range is chosen to give an optimal SNR value, which was calculated to be around 0.7 and correspondingly the fidelity was found to be around 70%.

The reason for $SNR < 1$ can be understood heuristically as follows. A single atom can process only one excitation of a transition per interaction time. Even if we consider that the control photon is completely absorbed by the atom, it can only scatter a single photon from the coherent probe field. As the noise of the coherent field is of the order of a photon, this displacement in its amplitude is not enough to allow us to distinguish between the cases of having $n = 0$ and $n = 1$ control photons. In fact, it can be seen that driving the 1–2 transition with the probe field actually reduces the excitation probability of the 0–1 transition (i.e. the incoming single photon is not completely absorbed by the atom), and thus we do not even reach the limit discussed above (see Fig. 4).

3.2. Beyond a single transmon

In order to overcome the limitations as discussed above, we look at using more than 1 transmon to displace the coherent probe over the limit set by the quantum noise. As a first step in this regard, we briefly review a convenient tool known as the (S, L, H) formalism [46,47] to derive the master equations for connected quantum systems. In this formalism, each

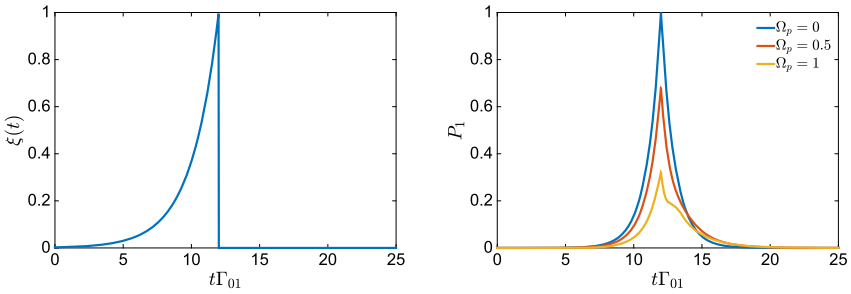

Fig. 4. Excitation probability of the 0–1 transition of a transmon: In the absence of a coherent probe field on resonance with 1–2 transition, the single photon in the control field is completely absorbed by the transmon, if we enclose it in a rising exponential wave-packet $\xi(t) = \Theta(t - T_{\text{ph}})\sqrt{\Gamma_{\text{ph}}}\exp\left(\frac{\Gamma_{\text{ph}}t}{2}\right)$ with $\Gamma_{\text{ph}} = \Gamma_{01}$. Switching on the probe field, reduces the maximum excitation probability, as can be seen in the second panel.

subsystem is described by a triplet $G \equiv (S, L, H)$, where S is the scattering matrix, L is the vector of coupling operators, and H is the Hamiltonian of the subsystem. Once the triplets are identified for each of the subsystems, the total triplet for the composite system can be written using the following products.

The series product $\triangleleft$ of the triplets describes feeding the output from one subsystem into another.

$$G_2 \triangleleft G_1 = \left(S_2 S_1, S_2 L_1 + L_2, H_1 + H_2 + \frac{1}{2\mathrm{i}}\left(L_2^\dagger S_2 L_1 - L_1^\dagger S_2^\dagger L_2\right)\right) \tag{12}$$

The concatenation product $\boxplus$ describes subsystems acting as independent parallel channels:

$$G_2 \boxplus G_1 = \left(\begin{pmatrix} S_2 & 0 \\ 0 & S_1 \end{pmatrix}, \begin{pmatrix} L_2 \\ L_1 \end{pmatrix}, H_2 + H_1\right) \tag{13}$$

The (S, L, H) formalism can also handle feedbacks. However, as we will not use them in this particular review, we refer the readers interested in feedbacks to the above references.

Using the above-defined products, we can write down the (S, L, H) triplet for the whole system

$$G_{\text{tot}} = \left(S_{\text{tot}}, \begin{pmatrix} L_1 \\ \vdots \\ L_n \end{pmatrix}, H_{\text{tot}}\right) \tag{14}$$

from which we can extract the corresponding master equation as

$$\dot{\rho} = -\mathrm{i}\,[H_{\text{tot}}, \rho] + \sum_{i=1}^{n} \mathcal{D}\,[L_i]\,\rho \tag{15}$$

The output from the ith channel is just given by L_i. The (S, L, H) triplet for the case of a single transmon with three levels in front of a mirror is

$$G_{\text{tr}} = \left(\mathbb{1}_2, \begin{pmatrix} L_{01} \\ L_{12} \end{pmatrix}, H_{\text{tr}}\right) \tag{16}$$

with the same Hamiltonian as in the previous section. The (S, L, H) triplets for the tunable cavity and the coherent probe in their corresponding rotating frames are

$$G_{\text{cav}} = (1, \sqrt{\kappa(t)}a, 0) \tag{17}$$

and

$$G_{\alpha_{\text{p}}} = (1, \alpha_{\text{p}}, 0) \tag{18}$$

With these triplets, we are now ready to look at different approaches with which we can connect different transmons. A first approach that is experimentally straightforward to implement is to couple many transmons with a transmission line one after the other (see Fig. 5). One can imagine two different scenarios in this case. The distance between the transmons could be much less than the wavelength of the incoming fields or it could be several factors higher. Both of these scenarios were analyzed in [39] and found not to be helpful for the problem of single-photon detection. The heuristic understanding for these is as follows. In case the transmons are closer than the transition wavelengths, the energy levels hybridize to form a larger atom with a different normalized coupling. In this case, we are back to the case of a single transmon, albeit with a different set of parameters. While this limitation could in principle be overcome by separating the transmons over larger

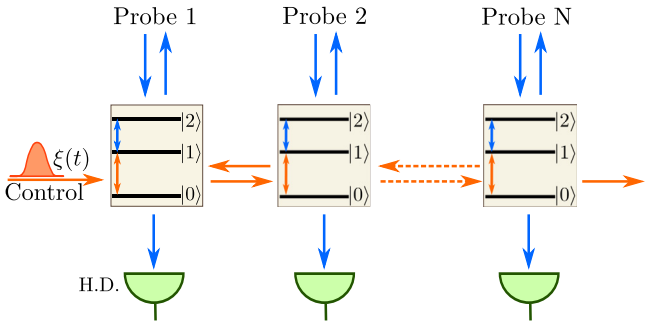

Fig. 5. Schematic setup of N transmons coupled with a transmission line. Each of the transmons is probed by a coherent field and the change in the reflected or transmitted amplitude is measured by a homodyne detector.

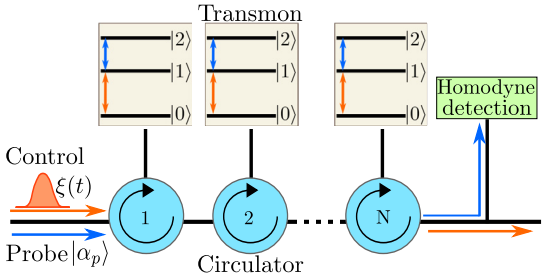

Fig. 6. Schematic setup of cascaded transmons for QND detection of microwave photons. Placing the transmons at the end of transmission lines and connecting them via circulators makes this a cascaded system where the fields travel unidirectionally.

distances, a Kramers–Kronig-type relation between the interaction and losses prevents any useful gain in the signal. To go beyond these limitations, we need a unidirectional coupling between the transmons, i.e. a cascaded setup as discussed in [40].

The setup considered is schematically shown in Fig. 6. We achieve an unidirectional flow of the fields by placing the transmons at the end of transmission lines (similar to having atoms in front of mirrors) and connecting them using microwave circulators. The master equation for this setup is derived as follows. Following the product rules in Eqs. (12) and (13), the (S, L, H) triplet for the setup consisting of N cascaded transmons with a tunable cavity as the photon source and a coherent probe of strength α_{p} is

$$\begin{aligned} G_{\mathrm{tot}} &= G_{\mathrm{tr}}^{(N)} \lhd \ldots \lhd G_{\mathrm{tr}}^{(k)} \lhd \ldots \lhd G_{\mathrm{tr}}^{(2)} \lhd G_{\mathrm{tr}}^{(1)} \lhd \left(G_{\mathrm{cav}} \boxplus G_{\alpha_{\mathrm{p}}}\right) \\ &= \left(\mathbb{1}_2, \begin{pmatrix} \sqrt{\kappa(t)}\, a + \Lambda_{01} \\ \alpha_{\mathrm{p}} + \Lambda_{12} \end{pmatrix}, H_{\mathrm{tot}}\right) \end{aligned} \tag{19}$$

where

$$\begin{aligned} H_{\mathrm{tot}} &= \sum_{j=1}^{N} H_{\mathrm{tr}}^{(j)} + \frac{1}{2\mathrm{i}}\sqrt{\kappa(t)}\left(\Lambda_{10}\, a - a^{\dagger}\Lambda_{01}\right) + \frac{1}{2\mathrm{i}}\left(\alpha_{\mathrm{p}}\,\Lambda_{21} - \alpha_{\mathrm{p}}^{*}\,\Lambda_{12}\right) \\ &\quad + \frac{1}{2\mathrm{i}}\sum_{j=1}^{N}\left(\sum_{k=j+1}^{N}\left(L_{10}^{(k)} L_{01}^{(j)} - L_{10}^{(j)} L_{01}^{(k)}\right)\right) + \frac{1}{2\mathrm{i}}\sum_{j=1}^{N}\left(\sum_{k=j+1}^{N}\left(L_{21}^{(k)} L_{12}^{(j)} - L_{21}^{(j)} L_{12}^{(k)}\right)\right) \end{aligned} \tag{20}$$

and the collective operators $\Lambda_{ij} = \sum_{k=1}^{N} L_{ij}^{(k)}$.

This gives the master equation (after some algebra) as

$$\begin{aligned} \dot{\rho} &= -\mathrm{i}\left[H_{\mathrm{eff}}, \rho\right] + \sum_{j=1}^{N}\left(\mathcal{D}\left[L_{01}^{(j)}\right] + \mathcal{D}\left[L_{12}^{(j)}\right]\right)\rho + \kappa(t)\mathcal{D}\left[a\right]\rho - \sqrt{\kappa(t)}\,\mathcal{C}\left[a, \Lambda_{01}\right]\rho \\ &\quad - \sum_{j=1}^{N}\sum_{k=j+1}^{N}\left(\mathcal{C}\left[L_{01}^{(j)}, L_{01}^{(k)}\right] + \mathcal{C}\left[L_{12}^{(j)}, L_{12}^{(k)}\right]\right)\rho \end{aligned} \tag{21}$$

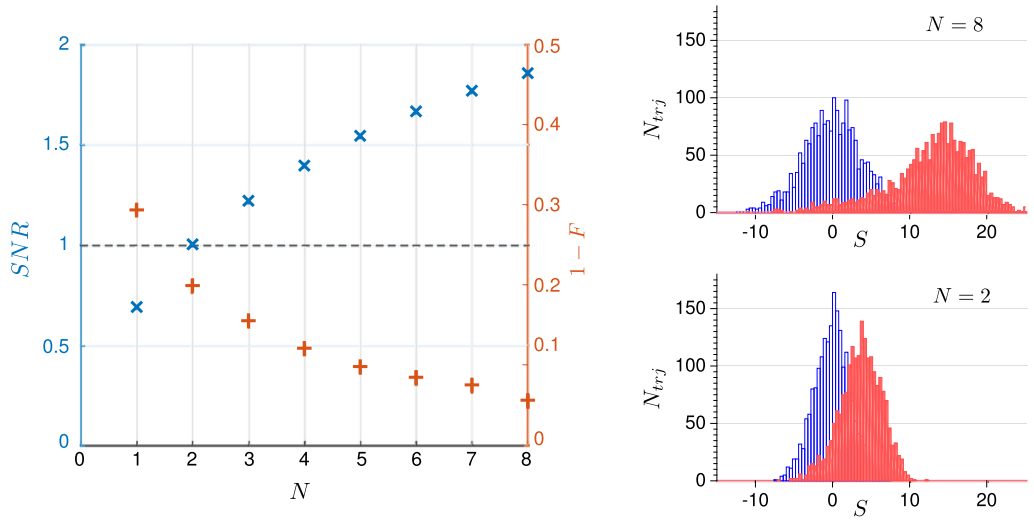

Fig. 7. Signal-to-noise ratio (SNR) and the fidelity of photon detection F as a function of N, the number of cascaded transmons. Both the control and the probe fields were taken to be on resonance with all of the transmons. The coupling of the individual transmons were tuned to optimize the SNR (refer to [40] for a full parameter list). The input photon was taken to be in a Gaussian wave packet. The insets show the signal distribution for $N = 2$ and $N = 8$ transmons. Note that for the case with an input control photon $n = 1$, the distributions deviate from a normal distribution with the increasing number of transmons, suggesting a memory effect. In such cases, we believe, the fidelity of photon detection becomes a better measure than the SNR.

where the effective Hamiltonian is $H_{\text{eff}} = \sum_{k=1}^{N} H^{(k)}$ with $H^{(k)} = -\Delta_{01}^{(k)} |0\rangle\langle 0|^{(k)} + \Delta_{12}^{(k)} |2\rangle\langle 2|^{(k)} + \Omega_{\text{p}}(L_{12}^{(k)} + L_{21}^{(k)})$. We have once again chosen the normalization for the probe field such that $\alpha_{\text{p}} = \Omega_{\text{p}} e^{i\pi/2}$, with Ω_{p} being a real number.

We once again numerically simulate the above equations and corresponding stochastic master equations to calculate the signal-to-noise ratio and the fidelity of photon detection. The main results are shown in Fig. 7. As we can see from the figure, the unidirectional coupling helps accumulate the effects from each one of the transmon and we can break-even the noise limit with $N = 2$ transmons. The resulting SNR can be fitted to a simple $\sqrt{N}$ curve, which would be the expected behavior if we had considered each one of the scattering events to be independent of one another. The results in Fig. 7 are once again for the ideal case of no dephasing in the transmons and with perfect homodyne detection. The setup also seems to work if we take into account some deviation from the ideal setup, though with reduced fidelities. We will not reproduce these results here and would refer the reader interested in full details to reference [40].

One of the main concerns in experimentally implementing the above setup is the need of circulators. Currently, these are bulky devices that are lossy and are off-chip. On-chip circulators [48–51] or other unidirectional wave-guides (such as quantum hall edge channels [52]) will make this scheme more attractive to implement. The performance of these setups could be further improved by using a cavity for the probe as shown in [41]. We will briefly review this in the next section.

3.3. Back to cavities

As mentioned in the introduction, early experiments in QND detection of microwave photons were done in cavity QED. A cavity field can interact with the atom over several cycles, as the interaction time between the atom and the cavity field is much less compared to the cavity lifetime. However, if we are interested in detecting an incoming photon from an arbitrary source (say from a different quantum node), we have to capture the photon in the cavity. To fully absorb the photon, the cavity needs to be of wide bandwidth and with strong coupling with the transmission line. High coupling, however, reduces the cavity lifetime, which degrades the performance of the photon-detection schemes. However, as the probe field is only an auxiliary field for detecting the incoming control photon, one could imagine having a cavity for the probe only, while the control photon is still an itinerant one. Such a setup (Fig. 8) was proposed and analyzed in [41].

We will first consider a single unit comprising a transmon with a cavity for the probe field. In the rotating frame of the input fields, the Hamiltonian can be written including the coherent drive as [41]

$$H = \Delta_{01} |1\rangle\langle 1| + (\Delta_{01} + \Delta_{12}) |2\rangle\langle 2| - i E(b - b^{\dagger}) - i g(b\sigma_{21} - b^{\dagger}\sigma_{12}) \tag{22}$$

where b is the annihilation operator of the probe cavity, E is the amplitude of the drive and g is the coupling strength between the cavity and the 1–2 transition. $\Delta_{01} = \omega_{01} - \omega_c$ is the detuning between the control field and the 0–1 transition, while $\Delta_{12} = \omega_{12} - \omega_{\text{cav}}$ is the detuning between the cavity field and the 1–2 transition. The master equation for this unit, using a cavity as a source of the control photon can be written as

$$\dot{\rho} = -i\,[H, \rho] + (\mathcal{D}[L_{01}] + \mathcal{D}[L_{12}])\,\rho + \kappa_a(t)\mathcal{D}[a]\,\rho + \kappa_b\mathcal{D}[b]\,\rho - \sqrt{\kappa_a(t)}\,\mathcal{C}[a, L_{01}]\,\rho \tag{23}$$

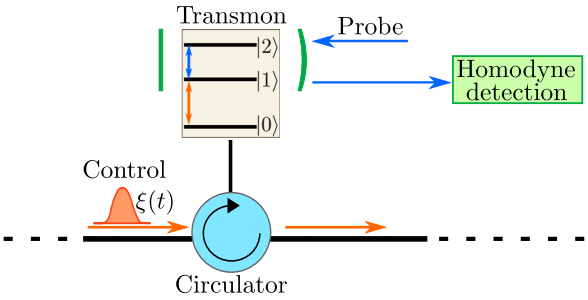

Fig. 8. Schematic setup of a transmon with a cavity for the probe field. The setup can be extended by adding more units (transmon + cavity) using circulators to get a cascaded setup. The field reflected from each cavity is measured using a homodyne detector to infer the presence of the control photon.

The field output from the probe cavity is measured using a homodyne detector and the corresponding homodyne current is

$$j(t)\,\mathrm{d}t = \sqrt{\kappa_b \eta}\left\langle \mathrm{e}^{-\mathrm{i}\phi} b + \mathrm{e}^{\mathrm{i}\phi} b^{\dagger} \right\rangle \mathrm{d}t + \mathrm{d}W(t) \tag{24}$$

In a similar way to the previous section, the performance of this setup was analyzed numerically and the fidelity F was shown to improve from 70% to 84%. This was achieved with the help of the cavity and by using an optimal linear filter $f(t)$ that takes the form of the expected homodyne current when the control field has a photon. The results also assume that the decay from the state $|2\rangle$ of the transmon into the transmission line can be suppressed to $\Gamma_{12} = 0.1\,\Gamma_{01}$. Using the usual transmon limit with $\Gamma_{12} = 2\,\Gamma_{01}$, the fidelity was found to be 81%. Further improvements were shown to be possible by cascading the units in a similar way to the previous section.

4. Summary

Microwave quantum optics using superconducting circuits, dubbed circuit QED, is an alternate approach for studying light–matter interaction that has been developing rapidly over the last few years. By confining the electromagnetic field to one dimension, a strong coupling regime can be reached in these setups that has already led to a plethora of interesting results. A single-photon detector in microwave regime will fill a major gap that would make these setups even more attractive for studying quantum optics and for developing quantum information technologies. The proposals we discussed in this article are aimed towards this goal. Especially, a QND single-photon detector would lead to several interesting applications, as discussed earlier. The setups (or similar ones) discussed for QND detection are close to their experimental realization and will become even more attractive with on-chip circulators and quantum limited amplifiers. We believe that new and exciting physics in microwave quantum optics will be studied using single-photon detectors in the near future.

Acknowledgement

We acknowledge financial support from the Swedish Research Council and the Knut and Alice Wallenberg Foundation.

References

[1] A. Einstein, Concerning an heuristic point of view toward the emission and transformation of light, Ann. Phys. 17 (1905) 132.
[2] H.-K. Lo, M. Curty, K. Tamaki, Secure quantum key distribution, Nat. Photonics 8 (2014) 595.
[3] M. Giustina, et al., Bell violation using entangled photons without the fair-sampling assumption, Nature 497 (2013) 227.
[4] E. Knill, R. Laflamme, G.J. Milburn, A scheme for efficient quantum computation with linear optics, Nature 409 (2001) 46.
[5] G.S. Buller, R.J. Collins, Single-photon generation and detection, Meas. Sci. Technol. 21 (2010) 12002.
[6] M.D. Eisaman, et al., Invited review article: single-photon sources and detectors, Rev. Sci. Instrum. 82 (2011).
[7] M. Mariantoni, et al., On-chip microwave Fock states and quantum homodyne measurements, Preprint, arXiv:cond-mat/0509737, 2005.
[8] M.P. da Silva, et al., Schemes for the observation of photon correlation functions in circuit QED with linear detectors, Phys. Rev. A 82 (2010) 43804.
[9] V.B. Braginskii, Y.I. Vorontsov, Quantum-mechanical limitations in macroscopic experiments and modern experimental technique, Sov. Phys. Usp. 17 (1975) 644.
[10] V.B. Braginskii, Y.I. Vorontsov, F.Y. Khalili, Quantum singularities of a ponderomotive meter of electromagnetic energy, J. Exp. Theor. Phys. 46 (1977) 705–706.
[11] K.S. Thorne, et al., Quantum nondemolition measurements of harmonic oscillators, Phys. Rev. Lett. 40 (1978) 667–671.
[12] W.G. Unruh, Quantum nondemolition and gravity-wave detection, Phys. Rev. B 19 (1979) 2888–2896.
[13] V.B. Braginskii, Y.I. Vorontsov, K.S. Thorne, Quantum nondemolition measurements, Science 209 (1980) 547–557.
[14] P. Grangier, J.A. Levenson, J.-P. Poizat, Quantum non-demolition measurements in optics, Nature 396 (1998) 537.
[15] A.M. Steane, Error-correcting codes in quantum theory, Phys. Rev. Lett. 77 (1996) 793.
[16] R. Ruskov, A.N. Korotkov, Entanglement of solid-state qubits by measurement, Phys. Rev. B 67 (1993) 241305.
[17] L.S. Bishop, et al., Proposal for generating and detecting multi-qubit GHZ states in circuit QED, New J. Phys. 11 (2009) 073040.
[18] R. Raussendorf, H.J. Briegel, One-way quantum computer, Phys. Rev. Lett. 86 (2001) 5188.
[19] G. Nogues, et al., Seeing a single photon without destroying it, Nature 400 (1999) 239.

[20] D.I. Schuster, et al., Resolving photon number states in a superconducting circuit, Nature 445 (2007) 515.
[21] C. Guerlin, et al., Progressive field-state collapse and quantum non-demolition photon counting, Nature 448 (2007) 889.
[22] H. Wang, et al., Measurement of the decay of a Fock states in a superconducting circuit, Phys. Rev. Lett. 101 (2008) 240401.
[23] B.R. Johnson, et al., Quantum non-demolition detection of single microwave photons in a circuit, Nat. Phys. 6 (2010) 663.
[24] Y. Yin, et al., Catch and release of microwave photon states, Phys. Rev. Lett. 110 (2013) 107001.
[25] J. Wenner, et al., Catching time-reversed microwave coherent state photons with 99.4% absorption efficiency, Phys. Rev. Lett. 112 (2014) 210501.
[26] E. Flurin, et al., Superconducting quantum node for entanglement and storage of microwave radiation, Phys. Rev. Lett. 114 (2015) 90503.
[27] G. Romero, J.J. García-Ripoll, E. Solano, Microwave photon detector in circuit QED, Phys. Rev. Lett. 102 (2009) 173602.
[28] G. Romero, J.J. García-Ripoll, E. Solano, Photodetection of propagating quantum microwaves in circuit QED, Phys. Scr. 2009 (2009) 14004.
[29] B. Peropadre, et al., Approaching perfect microwave photodetection in circuit QED, Phys. Rev. A 84 (2011) 063834.
[30] Y.F. Chen, et al., Microwave photon counter based on Josephson junctions, Phys. Rev. Lett. 107 (2011) 217401.
[31] A. Poudel, R. McDermott, M.G. Vavilov, Quantum efficiency of a microwave photon detector based on a current-biased Josephson junction, Phys. Rev. B 86 (2012) 174506.
[32] L.C.G. Govia, et al., Theory of Josephson photomultipliers: optimal working conditions and back action, Phys. Rev. A 86 (2012) 32311.
[33] L.C.G. Govia, et al., High-fidelity qubit measurement with a microwave-photon counter, Phys. Rev. A 90 (2014) 62307.
[34] K. Koshino, K. Inomata, Z. Lin, Y. Nakamura, T. Yamamoto, Theory of microwave single-photon detection using an impedance-matched Λ system, Phys. Rev. A 91 (2015) 43805.
[35] K. Koshino, Z. Lin, K. Inomata, T. Yamamoto, Y. Nakamura, Dressed-state engineering for continuous detection of itinerant microwave photons, Phys. Rev. A 93 (2016) 23824.
[36] K. Inomata, et al., Single microwave-photon detector using an artificial Λ-type three-level system, Preprint, arXiv:1601.05513, 2016.
[37] J. Koch, et al., Charge-insensitive qubit design derived from the Cooper pair box, Phys. Rev. A 76 (2007) 042319.
[38] I.-C. Hoi, et al., Giant cross Kerr effect for propagating microwaves induced by an artificial atom, Phys. Rev. Lett. 111 (2013) 053601.
[39] B. Fan, et al., Breakdown of the cross-Kerr scheme for photon counting, Phys. Rev. Lett. 110 (2013) 053601.
[40] S.R. Sathyamoorthy, et al., Quantum nondemolition detection of a propagating microwave photon, Phys. Rev. Lett. 112 (2014) 093601.
[41] B. Fan, et al., Nonabsorbing high-efficiency counter for itinerant microwave photons, Phys. Rev. B 90 (2014) 035132.
[42] J.E. Gough, M.R. James, H.I. Nurdin, J. Combes, Quantum filtering for systems driven by fields in single-photon states or superposition of coherent states, Phys. Rev. A 86 (2012) 043819.
[43] M. Lax, Quantum noise, IV: quantum theory of noise sources, Phys. Rev. 145 (1966) 110.
[44] H.M. Wiseman, G.J. Milburn, Quantum Measurement and Control, Cambridge University Press, 2010.
[45] H.J. Carmichael, An Open Systems Approach to Quantum Optics, Springer-Verlag, 1993.
[46] J. Gough, M.R. James, Quantum feedback networks: Hamiltonian formulation, Commun. Math. Phys. 287 (2009) 1109.
[47] J. Gough, M.R. James, The series product and its application to quantum feedforward and feedback networks, IEEE Trans. Autom. Control 54 (2009) 2530.
[48] J. Koch, et al., Time-reversal-symmetry breaking in circuit-QED based photon lattices, Phys. Rev. A 82 (2012) 043811.
[49] J. Kerckhoff, et al., On-chip superconducting microwave circulator from synthetic rotation, Rev. Phys. Appl. 4 (2015) 34002.
[50] K.M. Sliwa, et al., Reconfigurable Josephson circulator/directional amplifier, Phys. Rev. X 5 (2015) 41020.
[51] A.C. Mahoney, et al., On-chip microwave quantum Hall circulator, Preprint, arXiv:1601.00634, 2016.
[52] T.M. Stace, C.H.W. Barnes, G.J. Milburn, Mesoscopic one-way channels for quantum state transfer via the quantum Hall effect, Phys. Rev. Lett. 93 (2004) 126804.